

Dynamics of Molecular Motors and Polymer Translocation with Sequence Heterogeneity

Yariv Kafri*, David K. Lubensky# and David R. Nelson*

* *Department of Physics, Harvard University, Cambridge, MA 02138 and*

*BioMaPS Institute, Rutgers University, Piscataway NJ 08854 and Bell
Laboratories, Lucent Technologies, Murray Hill, NJ 07974*

Abstract

The effect of sequence heterogeneity on polynucleotide translocation across a pore and on simple models of molecular motors such as helicases, DNA polymerase/exonuclease and RNA polymerase is studied in detail. Pore translocation of RNA or DNA is biased due to the different chemical environments on the two sides of the membrane, while the molecular motor motion is biased through a coupling to chemical energy. An externally applied force can oppose these biases. For both systems we solve lattice models exactly both *with and without disorder*. The models incorporate explicitly the coupling to the different chemical environments for polymer translocation and the coupling to the chemical energy (as well as nucleotide pairing energies) for molecular motors. Using the exact solutions and general arguments we show that the heterogeneity leads to anomalous dynamics. Most notably, over a range of forces around the stall force (or stall tension for DNA polymerase/exonuclease systems) the displacement grows sublinearly as t^μ with $\mu < 1$. The range over which this behavior can be observed experimentally is estimated for several systems and argued to be detectable for appropriate forces and buffers. Similar sequence heterogeneity effects may arise in the packing of viral DNA.

I. INTRODUCTION

The dynamics of many single molecule experiments can be described in terms of a “particle” moving along a one-dimensional substrate. For example, polymer translocation through a narrow pore can be parameterized by the number of monomers threaded through the pore. The motion of molecular motors such as kinesins, dyneins, myosin, helicase, DNA polymerase, exonuclease and RNA polymerase can be described by the location of the motor on the one-dimensional substrate (microtubules, actin filaments, DNA and mRNA) on which they move. Similarly, the packing of a newly replicated DNA or RNA in viruses may be described by the molecular weight of the packed genome. These systems have been a subject of much experimental (Bates et al., 2003; Henrickson et al., 2000; Howard, 2001; Kasianowicz et al., 1996; Maier et al., 2000; Meller, 2003; Meller et al., 2001; Smith et al., 2001; Visscher et al., 1999; Wang et al., 1998; Wuite et al., 2000) and theoretical attention (Bhattacharjee and Seno, 2003; Bustamante et al., 2001; Chuang et al., 2002; Fisher and Kolomeisky, 1999; Flomenbom and Klafter, 2003, 2004; Goel et al., 2003; Jülicher et al., 1997; Jülicher and Bruinsma, 1998; Kolomeisky and Fisher, 1999; Lattanzi and Maritan, 2001,?, 2002; Lubensky and Nelson, 1999; Magnasco, 1993; Muthukumar, 2001; Prost et al., 1994; Sung and Park, 1996; Zandi et al., 2003).

Under most conditions the motion of the coordinate describing the system is biased in one direction. The bias in the case of molecular motors and packing of newly replicated viral genomes is due to a chemical process such as ATP (or more generally, NTP) hydrolysis, while for polymer translocation it can be generated by the different chemical environments on the two sides of the pore. For translocating single stranded DNA, such a bias could be provided by adding, for example RecA (Hegner et al., 1999) or other single stranded binding proteins (which do not pass through the pore) to the solution on one side of the membrane. Single molecule experiments allow another source of bias to be introduced into the system, namely an externally applied force F . This has been done, for example, by attaching a bead to a molecular motor (Visscher et al., 1999) or to the end of the genome which is packed into the viruses (Smith et al., 2001) and pulling on it using optical tweezers. Similarly, charged polymers have been translocated using an externally applied electric field (Meller et al., 2001). An interesting variant on these experiments is the single molecule measurements of Wuite et al. (Wuite et al., 2000) on DNA polymerase, which converts NTPs (nucleotide tri-

phosphates) into a ligated chain of nucleotides via complementary base pairing (Maier et al., 2000). Wuite et al. apply a force F' not to the motor itself, but instead across the ends of the ssDNA/dsDNA complex to create a *tension* across the substrate on which the molecular machine operates. Beyond a critical tension F'_c of order of 40 pN, the motor goes backward and turns into an exonuclease. The severe stretching of the backbone of the complementary DNA strand for $F' > F'_c$ presumably makes further conversion of NTPs unfavorable and causes removal of nucleotides by the motor to be favored. Forward and reverse motion of this enzyme are believed to be associated with different active sites (Doubl  e et al., 1998).

Most theoretical treatments of these systems have assumed homogeneous (or at least periodic) systems. Independent of the microscopic details, such problems can be described at long times by a random walker moving along a tilted potential or, equivalently, a biased random walker. For molecular motors such as kinesins, dyneins or myosins the assumption of homogeneity is indeed, in most experiments, entirely appropriate. However, in other cases the motion is along a one-dimensional *disordered* substrate. This is the case, for example, for RNA polymerases, exonuclease and DNA polymerases, helicases, the motion of ribosomes along mRNA, the translocation of RNA or DNA through a pore, and the packing of a viral genome. In all these systems the one dimensional substrate reflects the heterogeneity of DNA or RNA, and leads to a modification of the coarse-grained effective potential in which the random walker describing the system moves. The potential now depends in a complicated way on the location along the substrate. Two examples of potential energy landscapes of particular interest to us here are *random energy* and *random forcing* energy landscapes. We define a *random energy* landscape to be any effectively one-dimensional potential with a mean slope and fluctuations in the value of the potential with a finite variance about this linear tilt. A *random forcing* energy landscape has an overall mean slope but with energy fluctuations which are themselves described by a random walk. In this case, the energy fluctuations about a linear tilt grow as the square root of the distance along the substrate. These two types of energy landscapes have been studied in detail in the statistical mechanics literature (Bouchaud et al., 1990; Derrida, 1983) and lead to strikingly different long time dynamics. In particular the random forcing energy landscape leads to behavior quite different from diffusion with drift when the overall tilt of the landscape is small, as discussed in detail below.

Recently, the effect of disorder in the form of defect sites in a ratchet model which locally

reverse the bias of molecular motors has been considered (Harms and Lipowsky, 1997), using the methods of (Jülicher et al., 1997). It was suggested that even though fluctuations in the microscopic potential are bounded, the resulting *effective* energy landscape is random forcing. Specifically, it was argued that when the defect concentration was large enough anomalous random force dynamics would appear. As pointed out in (Lubensky and Nelson, 2002) heterogeneity in base pairing energies also leads to a random force landscape in the context of DNA unzipping.

In this paper we study the effect of sequence heterogeneity in both polymer translocation and molecular motors in detail for an exactly solvable class of simple lattice models. We consider both systems in the context of single molecule experiments that apply an external force pulling back on the polymer or the motor, which in the absence of this force are biased to move in one direction. We introduce microscopic models for both systems which can be solved *exactly* both with and without disorder. A generalization of our motor model, discussed in Section V and Appendix D, can also be used as a very simple model of the DNA polymerase/exonuclease experiments of Ref. (Wuite et al., 2000). One can also consider closely related models of the packing of a viral genome. In this case there is an extra source of bias due to the energetic cost of packing the DNA inside the virus. The externally applied force acts in conjunction with this bias while the motor acts against both. The details are very similar to the cases discussed here, with the exception that the energy cost of forcing the DNA into the capsid does not necessarily vary strictly linearly with the amount of DNA that has entered. We do not include a separate discussion of this interesting system.

We show that sequence heterogeneity of single stranded DNA or RNA and heterogeneous base pairing energies have a dramatic effect on the dynamics of both systems. For a homogeneous substrate and no chemical bias, the average velocity changes monotonically through zero as the external force is varied, changing sign as the force reverses direction (see Fig. 1(a)). When a chemical bias (which we take to act in the direction opposing the force) is present, the scenario is similar with the velocity changing sign at a stall force, F_s , which depends on the degree of chemical bias (see Fig. 1(b)). In contrast, the combination of a disordered substrate and a chemical bias produces very different behavior for both systems. In this case we show that generically disorder introduces a random forcing effective energy landscape which is responsible for the anomalous dynamics. Similar to the observation of Harms and Lipowsky (Harms and Lipowsky, 1997) a random forcing landscape is gener-

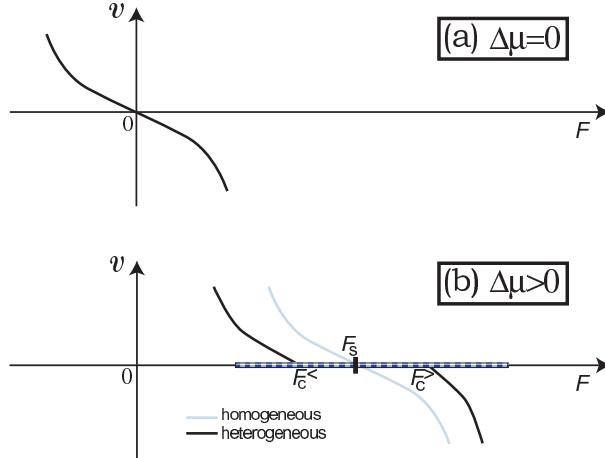


FIG. 1 Schematic behavior of the drift velocity at long times for homogeneous and heterogeneous systems as a function of the applied force, where a positive force *resists* the chemically favored direction of motion. It is assumed that chemical forces (such as ATP hydrolysis or chemical binding on one side of a pore) lead to a positive velocity in the absence of a force. (a) No externally applied chemical bias ($\Delta\mu = 0$). (b) A finite chemical bias ($\Delta\mu > 0$), where the light line corresponds to homogeneous or periodic environments and the solid line refers to heterogeneous environments. The anomalous dynamics ($\langle x(t) \rangle \sim t^\mu$, with $\mu < 1$) arises in the vicinity of what would be the stall force, F_s , for the homogeneous system. For $F_c^< < F < F_c^>$, the effective velocity depends on the width of the time averaging window, and tends to zero as the width of the window goes to infinity. The striped line denotes the region where anomalous diffusion is also present.

ated even if we neglect an explicit contribution (Lubensky and Nelson, 2002) from random base pairing energies. We discuss three different dynamical regimes which arise due to this landscape as the externally applied force is varied. The most notable transition arises in the velocity of the random walker describing the system. Specifically, we find that there are critical values of the force $F_c^>$ and $F_c^<$ such that for any force between these values the velocity is zero in the sense that the average particle position $\langle x(t) \rangle$, where $\langle \dots \rangle$ denotes an average over thermal fluctuations, increases as a *sublinear* power of time. We also discuss an even broader range of forces where the diffusion is anomalous (see Fig. 1(b)). The transition points between the different types of long-time dynamics can be calculated exactly for the simple models studied here.

Under special conditions a random energy landscape is also possible. In this case the expected behavior as a function of force is similar to a homogeneous system: The potential

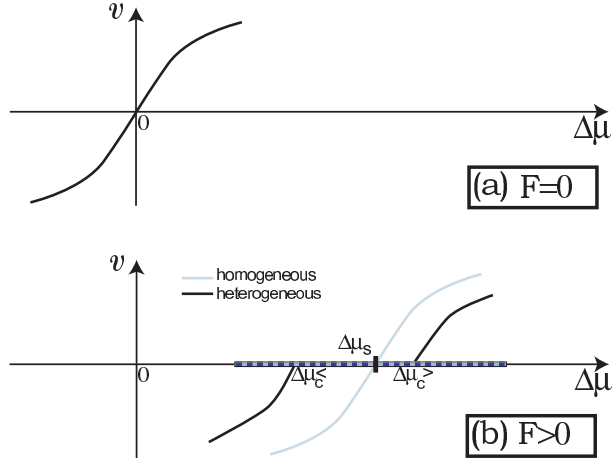


FIG. 2 Schematic behavior of velocity for homogeneous and heterogeneous systems as a function of the chemical bias $\Delta\mu$. (a) No externally applied force. (b) A finite externally applied force for homogeneous (light line) and heterogeneous (solid line) substrates. The anomalous dynamics arises in the vicinity of what would be the stall chemical bias, $\Delta\mu_s$, for the homogeneous system. As in Fig. 1, the striped line denotes the region where anomalous diffusion is present.

fluctuations simply renormalize the drift velocity and diffusion constant at long times. That is, as the applied force is varied the behavior is similar to that of a homogeneous system with no chemical bias. Provided that random contributions to the energy landscape not associated with simple conversion of chemical energy can be neglected, random energy models describe the dynamics in the absence of chemical bias (see Fig. 1(a)) on heterogeneous substrates.

An alternative way to observe the anomalous dynamics is by holding the external force constant and varying the chemical bias. This can be done by changing the concentration of, say, nucleotide triphosphates for molecular motors, or by changing the concentration of the polymer binding protein in one chamber for polymer translocation experiments. In this case, when the force is held at zero, the velocity changes monotonically in tandem with the chemical bias (see Fig. 2(a)). However, when the external force is held constant at a non-zero value, a region with anomalous dynamics appears as the chemical bias is varied (see Fig. 2(b)). Between two values of the chemical bias $\Delta\mu_c^<$ and $\Delta\mu_c^>$, the displacement of the particle with time is again sublinear, in contrast to the same experiment performed on a homogeneous substrate. As illustrated in Fig. 2(b) the velocity is then a monotonic function of the chemical bias, changing sign at a stalling chemical bias $\Delta\mu_s$. A summary of the qualitative behavior of the velocity as function of both the chemical bias $\Delta\mu$ and the

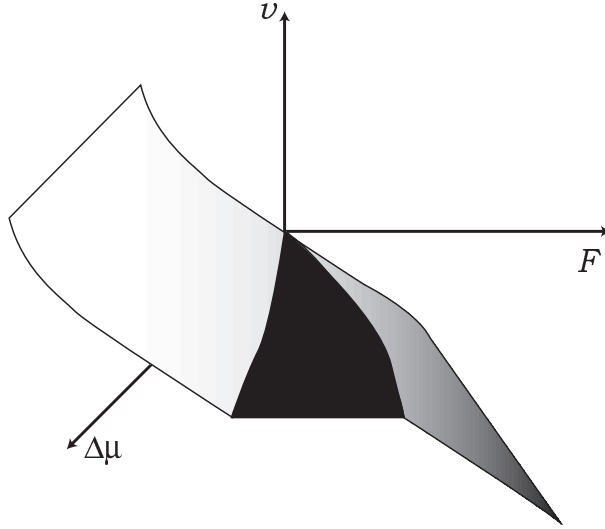


FIG. 3 The dependence of the velocity on the chemical bias $\Delta\mu$ and the external force F . We neglect for simplicity contributions to a random force landscape (such as fluctuations in base pairing energies) which may be present even for $\Delta\mu = 0$. Here it is assumed that the chemical bias always act in the direction opposing the force. The black wedge denotes a region of sublinear drift with time, i.e., effectively zero velocity.

external force F is shown in Fig. 3. It is worth noting that there is no region of sublinear displacement when $\Delta\mu = 0$ because the energy landscape is then random energy rather than random forcing, whereas when $F = 0$, there is still a random forcing landscape everywhere except exactly at stalling, but the randomness is too small in the vicinity of $\Delta\mu = 0$ to cause anomalous dynamics.

To keep the discussion simple, Fig. 3 neglects contributions to a random forcing landscape other than those produced by the simple conversion of chemical energy along an inhomogeneous track. Additional random forcing contributions will arise from, e.g., base pairing energies in the case of helicases, which open up DNA strands or DNA polymerases and exonucleases, which add or delete complementary base pairs. Motors, such as RNA polymerases and ribosomes produce trailing strands of mRNA and protein respectively. Since these products are themselves heteropolymers, composed of monomers which interact differently with the solvent, here too we would expect additional contributions to a random forcing landscape. Such effects will only accentuate the anomalous dynamics which is the subject of this paper.

Before concluding this introduction, we should emphasize our perspective on the models

of polynucleotide translocation and molecular motors studied here. In an effort to obtain simple, soluble models which incorporate heterogeneity, we intentionally neglect important molecular details such as those which describe the detailed pore interactions of the translocating nucleotides or distinguish the biological role of motors such as helicases, DNA polymerase and exonucleases, RNA polymerase, etc. The motors mentioned above perform important specialized functions such as opening double stranded DNA, polymerization and depolymerization or creating messenger RNA while moving along heterogeneous tracks. Such functions are incorporated into our model simply by adding an explicit (position-dependent) chemical force to the energy landscape. More sophisticated attempts to get molecular details right (see, e.g., Refs. (Goel et al., 2003),(Simon et al., 1992) and (Betterton and Jülicher, 2003)) serve a valuable purpose, which can be important for modelling some aspects of the dynamics on various time scales. However, incorporation of sequence heterogeneity, neglected in most previous modelling efforts, is nevertheless crucial to correctly describe the anomalous long time dynamics (e.g., $\langle x(t) \rangle \sim t^\mu$ with $\mu < 1$) near the stall forces in these systems. Otherwise, we expect simple diffusion with drift (similar to what we find here for homogeneous models or a random energy landscape) at long times. We do not expect the multiple intermediate states and numerous rate constants of more sophisticated models to change our predictions of heterogeneity-induced anomalous dynamics at long times.

The paper is organized as follows: In Section II, to establish notation and provide a context for the rest of the paper, we discuss the homogeneous models for polymer translocation and molecular motors in some detail. In Section III the effect of the heterogeneity on the energy landscape is introduced. Section IV discusses the resulting dynamical behavior and the exact location of the transition points within the models. Finally, Section V estimates the experimental range over which the anomalous dynamics may be observed for a few representative biological systems and discusses the effect of finite time experiments on the shape of the velocity-force curve.

II. HOMOGENEOUS MODELS

Before turning to heterogeneous systems we first define microscopic models for both homogeneous polymer translocation and molecular motors. The simplicity of both models allows for their exact solution. Dynamics in heterogeneous systems will be treated in Sections

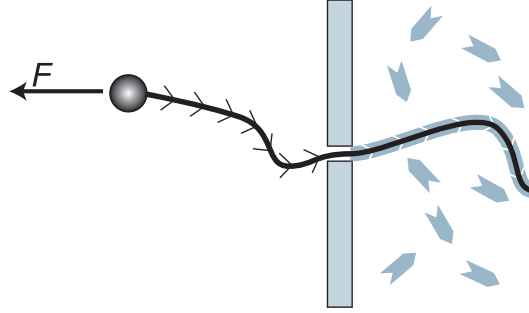


FIG. 4 Schematic picture of the polymer translocation experimental setup considered. A polymer is biased to move through the pore by a solution of binding proteins in the right chamber. A bead exerts a force in the opposite direction. The arrows reflect the lack of inversion symmetry in, e.g., single stranded DNA or RNA.

III and IV.

A. Polymer Translocation

An idealized experimental setup is shown schematically in Fig. 4. A polymer is threading through a narrow pore located on a two dimensional membrane which separates two chemically distinct solutions. For concreteness we consider the right side as containing a polymer binding protein which is absent in the left hand side. In addition, a bead, through which a resisting force is exerted on the polymer, is connected to the left end of the polymer. A model of this kind has been discussed by P. Nelson (Nelson, 2003) as a simple example of stochastic ratchet-like dynamics in biological systems (see also (Peskin et al., 1993)). Alternatively a force could be applied via an external electric field acting across the pore on a charged polymer (Kasianowicz et al., 1996).

A convenient representation of the system is through a one-dimensional random walker located at a coordinate x which represents the length of the polymer that has translocated to the righthand side. The conditions under which the full three-dimensional, multi-species problem can be simplified are reviewed below. The dynamics of the random walker is governed by the interaction of the polymer with the pore, the binding of the protein in the right chamber, and the externally applied force.

Before turning to a specific microscopic model consider the general form of the potential experienced by the random walker due to all these interactions. Because we neglect sequence

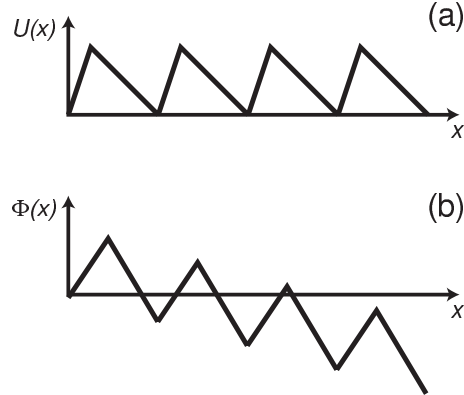


FIG. 5 (a) The periodic potential due to pore interactions with a translocating polymer without inversion symmetry. (b) The tilt of this potential generated by a combination with the binding protein and the external force.

heterogeneity in this section, the energy due to interactions with the pore, $U(x)$, is some periodic function with a period given by the size of a monomer. An example is the sawtooth or ratchet potential shown in 5(a). This type of potential accounts for an energetic barrier for translocation through the pore. The lack of inversion symmetry reflects, for example, the difference in passing single stranded DNA or RNA in the $3' \rightarrow 5'$ direction through the pore as opposed to the reverse. The energy due to the interaction with the polymer binding protein is however very different and has the form $-F_\mu x$, growing linearly with x . Thus the energy decreases as the polymer translocates to the righthand side. The value of F_μ is governed by the chemical potential difference per monomer, $\Delta\mu$, of the polymer in the solutions on the righthand and lefthand sides. This chemical potential difference is a function of the protein concentration and its binding energy to the polymer (a more detailed description of F_μ for the microscopic model discussed below is presented in Appendix A). Finally, the backward force applied on the bead leads to a contribution to the energy of the form Fx . Upon collecting together these contributions, the total potential experienced by the random walker, $\Phi(x)$, is given by

$$\Phi(x) = U(x) - (F_\mu - F)x . \quad (1)$$

As is evident from the effective energy landscape shown in Fig. 5(b), the random walker is moving in a periodic potential with an overall slope which depends on the protein concentration and binding energy as well as the external force. Such a potential leads on long time scale and large length scales to motion which is diffusion superimposed on an overall drift

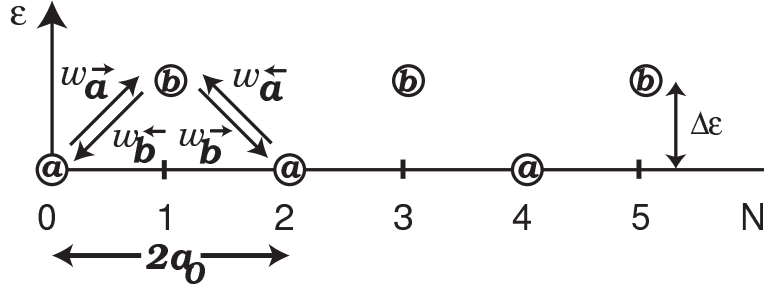


FIG. 6 Graphical representation of a simplified model for polymer translocation or molecular motors. These two cases are distinguished by the choice of rate constants (see text). The distinct even and odd sublattices are denoted by a and b respectively.

velocity. Thus, the average location of the particle $\langle x \rangle$ behaves as $\langle x \rangle = vt$ while the mean square fluctuations about this drift behave as $\langle x^2 \rangle - \langle x \rangle^2 = 2Dt$, where v and D depend on $F_\mu - F$ and the details of the ratchet potential (see, e.g., (Lubensky and Nelson, 1999)). Here, the brackets $\langle \dots \rangle$ represent an average over thermal fluctuations.

We emphasize that our simplified description in terms of a single coordinate x that diffuses and drifts in a one-dimensional energy landscape is valid only when the translational motion of the polymer backbone through the pore is the slowest process in the problem (Lubensky and Nelson, 1999). In particular, this model assumes that the translocating polymer is not so long that the relaxation times in the cis (left) or trans (right) chambers exceed the diffusion time for the backbone through the pore. This simplified model is also inadequate if the polymer can become bound to the pore interior for long periods, as recent experiments suggest occurs for one of the best studied polymer-pore systems (Bates et al., 2003). In this case, x will still undergo biased diffusion on long enough time scales, but its velocity and diffusion coefficient will no longer be determined by a simple potential $U(x)$. Finally, the effect of binding proteins can be captured by a single free energy parameter $\Delta\mu$ only when their binding and unbinding kinetics are sufficiently fast. The opposite limit, in which proteins bind irreversibly, but slowly, to the polymer, has also received attention (Peskin et al., 1993; Simon et al., 1992; Sung and Park, 1996), but we will not consider it further here.

We now define a simplified microscopic model for the motion of a random walker in such a potential. Our model is in the spirit of those analyzed for motor proteins in (Fisher and Kolomeisky, 1999; Kolomeisky and Fisher, 1999) (see also Sec. II.B),

and allows exact results for the diffusion and drift on long times. In the language of (Fisher and Kolomeisky, 1999; Kolomeisky and Fisher, 1999) our model is a $n = 2$ model corresponding to a motor with just two internal states. More importantly, our model generalizes naturally to a *heterogeneous* version (see Section III) for which exact results are also possible. We allow x to assume a discrete set of values x_m , where $m = 0, 1, 2, \dots$ labels distinct a (even) and b (odd) sites. We can allow different distances between $x_{m+1} - x_m$ and $x_{m+2} - x_{m+1}$ but require $x_{m+2} - x_m = 2a_0$ which we assume for simplicity is the size of the polymer unit which accommodates a single adsorbed protein. For a homopolymer the interactions with the pore are some periodic function with a period which we can take to be $2a_0$. To model this situation we take odd labelled sites to have a higher energy than even labelled sites. The arrangement is shown schematically in Fig. 6. Even sites have an energy $\varepsilon = 0$ while odd sites (corresponding roughly to the peaks in the ratchet potential of Fig. 5) have a higher energy $\varepsilon = \Delta\varepsilon$. Also, indicated in the figure are the hopping rates which describe the dynamics of the random walker. The detailed balance condition (in temperature units such that $k_B = 1$) is satisfied by

$$\begin{aligned}
w_a^{\rightarrow} &= \omega e^{-\Delta\varepsilon/T - f/2T} \\
w_b^{\leftarrow} &= \omega e^{f/2T} \\
w_a^{\leftarrow} &= \omega' e^{(-\Delta\mu - \Delta\varepsilon + f/2)/T} \\
w_b^{\rightarrow} &= \omega' e^{-f/2T} .
\end{aligned} \tag{2}$$

Because of the lack of reflection symmetry in the translocating DNA or RNA (for our model this asymmetry could be represented by taking $x_1 - x_0 \neq x_2 - x_1$), we expect the intrinsic hopping rates to be unequal, $\omega \neq \omega'$. The bias induced by the interaction of individual monomers with the reservoir of proteins on one side of the pore has been accounted for by the chemical potential difference $\Delta\mu$. A more detailed discussion of the dependence of $\Delta\mu$ on the protein binding energy and its concentration is given in Appendix A. The effect of the applied force is included through the parameter $f = Fa_0$. Note that the bias controlled by $\Delta\mu > 0$ arises only for steps from odd to even sites since a protein is assumed to bind only to a whole monomer. As pointed out, in (Kolomeisky and Fisher, 1999), other f -dependences of the rates consistent with detailed balance are possible. We shall be content with the simple one displayed in Eq. 2 which corresponds to choosing $x_1 - x_0 = x_2 - x_1$.

To show that this microscopic model embodies an effective potential of the form (1), we

eliminate the odd-numbered sites. This elimination can be accomplished by formally solving the equations of motion for the odd sites, substituting into the remaining even site equations, and taking the long-time limit (see Appendix B). Alternatively we can invoke detailed balance and consider an effective energy difference $\Delta E = E(m+2) - E(m)$ between site $m+2$ and m where m is even. Upon setting

$$\frac{W_{m,m+2}}{W_{m+2,m}} \equiv e^{(E(m+2)-E(m))/T}, \quad (3)$$

where $W_{n,m}$ is the effective transition rate between site m and n , we have

$$\begin{aligned} \Delta E &= E(m+2) - E(m) \\ &= T \ln \left(\frac{w_a^{\leftarrow} w_b^{\leftarrow}}{w_a^{\rightarrow} w_b^{\rightarrow}} \right). \end{aligned} \quad (4)$$

Use of the rates (2) leads to

$$\Delta E = -\Delta\mu + 2f \quad (5)$$

as one would expect. Note that when the force vanishes ($f = 0$) and the chemical potential gradient $\Delta\mu = 0$ one has $\Delta E = 0$ and no net motion is generated. More generally, an effective tilted potential of the form (1) is generated, with $\Delta\mu > 0$ causing a drift of the polymer to the right. The external force on the left can reduce or even reverse the overall slope. Such a potential inserted into microscopic rate equations for the even sites (see Appendix B) is well known to lead to diffusion with drift on long time scales and large length scales.

In fact, for this model using the results of (Derrida, 1983) and following (Fisher and Kolomeisky, 1999; Kolomeisky and Fisher, 1999) one can calculate the velocity and diffusion constant exactly. After some lengthy calculations, one obtains for the velocity

$$v = 2a_0 \frac{w_a^{\rightarrow} w_b^{\rightarrow} - w_a^{\leftarrow} w_b^{\leftarrow}}{w_a^{\rightarrow} + w_a^{\leftarrow} + w_b^{\rightarrow} + w_b^{\leftarrow}}. \quad (6)$$

The diffusion constant of the model is given by

$$D = 2a_0^2 \frac{(w_a^{\leftarrow} w_b^{\leftarrow} + w_a^{\rightarrow} w_b^{\rightarrow}) + 8w_a^{\leftarrow} w_b^{\leftarrow} w_a^{\rightarrow} w_b^{\rightarrow}}{(w_a^{\leftarrow} + w_b^{\leftarrow} + w_a^{\rightarrow} + w_b^{\rightarrow})^3} K, \quad (7)$$

with

$$\begin{aligned} K &= (w_a^{\leftarrow})^2 + (w_b^{\leftarrow})^2 + (w_a^{\rightarrow})^2 + (w_b^{\rightarrow})^2 \\ &+ 2(w_a^{\rightarrow} w_a^{\leftarrow} + w_b^{\rightarrow} w_b^{\leftarrow} + w_a^{\leftarrow} w_b^{\rightarrow} + w_a^{\rightarrow} w_b^{\leftarrow}). \end{aligned} \quad (8)$$

It is interesting to set $f = 0$ and consider the limit of $\Delta\mu/T \ll 1$ (small chemical bias, no external force) and the limit $\Delta\mu/T \rightarrow \infty$ and $\Delta\mu \gg \Delta\varepsilon$ (large chemical bias, no external force). When $\Delta\mu/T \ll 1$ the velocity takes the linear response form

$$v = \frac{2a_0\omega\omega'e^{-\Delta\varepsilon/T}}{(\omega + \omega')(1 + e^{-\Delta\varepsilon/T})} \frac{\Delta\mu}{T} \quad (9)$$

In the limit of $\Delta\mu/T \rightarrow \infty$ and $\Delta\mu \gg \Delta\varepsilon$, the velocity saturates at v_{\max} , with

$$v_{\max} = 2 \frac{\omega\omega'}{\omega + e^{\Delta\varepsilon/T}(\omega + \omega')} . \quad (10)$$

In both cases the velocity is a decreasing function of $\Delta\varepsilon$, as one might expect because the rate limiting step in this simple polymer translocation model is the energetic barrier as each successive segment passes through the pore potential.

For the diffusion constant one finds similarly in the limit $\Delta\mu/T \ll 1$

$$D = 4a_0^2 \frac{\omega\omega'e^{-\Delta\varepsilon/T}}{(\omega + \omega')(1 + e^{-\Delta\varepsilon/T})} - 2a_0^2 \frac{\Delta\mu}{T} \frac{(\omega(1 + e^{-\Delta\varepsilon/T}) + \omega'(1 - e^{-\Delta\varepsilon/T}))}{(\omega + \omega')^2(1 + e^{-\Delta\varepsilon/T})^2} . \quad (11)$$

Like the velocity, in this regime the diffusion constant decreases as $\Delta\varepsilon$ increases. Note that the diffusion constant decreases when $\Delta\mu$ increases. This behavior arises since the rate of backward steps decreases as $\Delta\mu$ increases. In the limit $\Delta\mu/T \rightarrow \infty$, and $\Delta\mu \gg \Delta\varepsilon$ we find that the diffusion constant saturates at

$$D_{\max} = a_0^2 \frac{2\omega\omega'((\omega + \omega')^2 e^{2\Delta\varepsilon/T} + \omega^2(1 + 2e^{\Delta\varepsilon/T}))}{(\omega + e^{\Delta\varepsilon/T}(\omega + \omega'))^3} , \quad (12)$$

which also decreases with $\Delta\varepsilon$. The diffusion constant again decreases as a function of $\Delta\varepsilon$ due to the rate limiting step of the passage through the pore.

B. Molecular Motors

A typical experimental setup is shown in Fig. 7. The motor attempts to move from the + end to the - end by utilizing the chemical energy stored in ATP or some other source of chemical energy. For RNA polymerase, this energy source would be the nucleotide triphosphates which are converted into mRNA (not shown). A force (say from an optical tweezer) pulls in the opposite direction to the motion generated by the ATP. In this section,

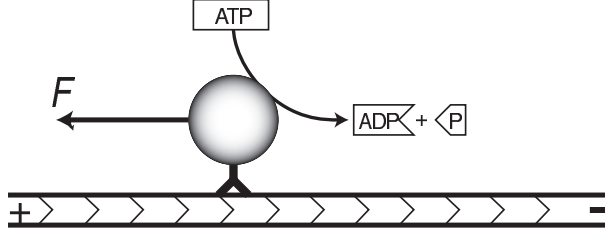


FIG. 7 Setup modelled. The motor is moving from the + end to the – end. A force is pulling on the motor in the opposite direction. Note that some of the specific biological examples considered in the text are more complicated and may be driven by energy sources other than ATP.

we focus primarily on models of relatively simple motors as in Fig. 7 and mention only in passing more complicated effects associated with motors such as helicases or RNAP.

Theoretical models of molecular motors (Jülicher et al., 1997) have demonstrated how an effective potential of the form (1) is generated as a result of the coupling to an energy source like ATP for a general class of periodic substrate potentials which lack inversion symmetry. Here we again introduce a simple model for a two level ratchet which is amenable to an exact solution, similar to an $n = 2$ version of the models of Fisher and Kolomeisky (Fisher and Kolomeisky, 1999; Kolomeisky and Fisher, 1999). Like the model for polymer translocation in Section A, this motor model will allow us to study the effect of heterogeneity. We first consider the homogeneous motor model in some detail.

We again consider a one-dimensional lattice where even sites have energy $\varepsilon = 0$ while odd sites have an energy $\varepsilon = \Delta\varepsilon$. The odd sites represent an “inchworm”-like walking which is facilitated by chemical energy released by, e.g., hydrolysis of ATP. The transition rates depicted in Fig. 6 now take a different form, namely

$$\begin{aligned}
 w_a^{\rightarrow} &= (\alpha e^{\Delta\mu/T} + \omega) e^{-\Delta\varepsilon/T - f/2T} \\
 w_b^{\leftarrow} &= (\alpha + \omega) e^{f/2T} \\
 w_a^{\leftarrow} &= (\alpha' e^{\Delta\mu/T} + \omega') e^{-\Delta\varepsilon/T + f/2T} \\
 w_b^{\rightarrow} &= (\alpha' + \omega') e^{-f/2T}.
 \end{aligned} \tag{13}$$

Note that there are two parallel channels for the transitions (Jülicher et al., 1997). The first, represented by contributions containing α and α' , arise from utilization of chemical energy. The second channel, represented by the terms containing ω and ω' , correspond to thermal transitions unassisted by the chemical energy. $\Delta\mu$ is given by the standard relation

(Howard, 2001),

$$\Delta\mu = T \left[\ln \left(\frac{[ATP]}{[ADP][P]} \right) - \ln \left(\frac{[ATP]_{\text{eq}}}{[ADP]_{\text{eq}}[P]_{\text{eq}}} \right) \right] \quad (14)$$

where the square brackets $[\dots]$ denote concentrations under experimental conditions and the $[\dots]_{\text{eq}}$ denote the corresponding concentrations at equilibrium. We have again assumed the external applied force f biases the motion in a particularly simple way. If the substrate lacks inversion symmetry, we have $\alpha' \neq \alpha$ and $\omega' \neq \omega$. As discussed in the introduction, in some cases an additional force arises from, e.g., base pairing energies in the case of helicases, DNA polymerase and exonucleases. Similarly an addition force arises also for motors such as RNA polymerase and ribosomes which produce trailing strands of mRNA or protein respectively. Here we ignore such contributions although they could easily be added in a simple way to the model through a redefinition of f through $f \rightarrow f + f_\mu$ where f_μ is the additional force. The model is formally similar to the model of polymer translocation, although the different functional form of $w_a^{\rightarrow}, w_b^{\leftarrow}, w_a^{\leftarrow}$ and w_b^{\rightarrow} has important consequences.

First we consider the effective energy landscape. To this end, we again eliminate the odd sites and describe the remaining dynamics in terms of an effective potential. This is the effective potential under which a random walker satisfying detailed balance would exhibit the same dynamics. From a formula similar to Eq. 3, one finds that $\Delta E = E(m+2) - E(m)$, where m is an even site, is given by

$$\begin{aligned} \Delta E &= T \ln \left(\frac{(\alpha + \omega)(\alpha' e^{\Delta\mu/T} + \omega')}{(\alpha e^{\Delta\mu/T} + \omega)(\alpha' + \omega')} \right) \\ &+ 2f \end{aligned} \quad (15)$$

where we have used the rates (13)

Note that when the external force $f = 0$ and the ATP/ADP+P chemical potential difference $\Delta\mu = 0$, one has $\Delta E = 0$ and no net motion is generated. Also, when there is directional symmetry in the transition rates $\alpha = \alpha', \omega = \omega'$ and $f = 0$ one has $\Delta E = 0$ even when $\Delta\mu \neq 0$. Absent this symmetry, chemical energy can be converted to motion and an effective tilted potential is generated. Although, these conditions are equivalent to those presented in (Jülicher et al., 1997; Prost et al., 1994) for continuum models, it is interesting to see them at work in the “minimal” model studied here (see also (Fisher and Kolomeisky, 1999) and (Kolomeisky and Fisher, 1999)). The effect of the externally applied force is simply to change the overall tilt in the potential.

For a motor on a homogeneous or periodic substrate the effective potential generated by the coupling to the chemical potential is thus qualitatively the same as that of a polymer translocating through a pore. Again on long time scales and large length scales the dynamics is just diffusion with drift. The equation for the velocity and diffusion constant are given by Eqs. 6,7,8 together with the rates displayed in Eq. 13.

As for the polymer translocation problem, it is interesting to consider various limits for the case $f = 0$. Using (13) we find in the limit of $\Delta\mu/T \ll 1$ a drift velocity

$$v = \frac{2a_0(\omega'\alpha - \omega\alpha')e^{-\Delta\varepsilon/T}}{(\alpha + \omega + \alpha' + \omega')(1 + e^{-\Delta\varepsilon/T})} \left(\frac{\Delta\mu}{T} \right) \quad (16)$$

Therefore, for small $\Delta\mu/T$, the velocity decreases as $\Delta\varepsilon$ increases. Note that even when $\Delta\mu \neq 0$, v vanishes for a symmetric substrate, i.e. for $\omega' = \omega$ and $\alpha' = \alpha$. A natural measure of the asymmetry of the potential is $\omega'\alpha/\omega\alpha'$. When this quantity is greater than one (less than one) a positive $\Delta\mu$ induces a motion to the right (left). This result remains valid to any order in $\Delta\mu$.

The maximum possible motor velocity v_{\max} is obtained in the limit $\Delta\mu/T \rightarrow \infty$ and $\Delta\mu \gg \Delta\varepsilon$, where

$$v_{\max} = 2a_0 \frac{\omega'\alpha - \omega\alpha'}{\alpha + \alpha'}. \quad (17)$$

In contrast to the previous regime and the polymer translocation problem, the velocity is insensitive to $\Delta\varepsilon$. Because of the injection of large amounts of external chemical energy, the barrier $\Delta\varepsilon$ no longer controls a rate limiting step.

For the diffusion constant of this model of molecular motors in the limit $\Delta\mu/T \ll 1$ we find

$$D = 4a_0^2 \frac{(\alpha + \omega)(\alpha' + \omega')e^{-\Delta\varepsilon/T}}{(\alpha + \omega + \alpha' + \omega')(1 + e^{-\Delta\varepsilon/T})} + a_0^2 \frac{\Delta\mu}{T} \frac{2e^{-\Delta\varepsilon/T}G}{(\alpha + \omega + \alpha' + \omega')^2(1 + e^{-\Delta\varepsilon/T})^2} \quad (18)$$

with

$$G = e^{-\Delta\varepsilon/T}(\alpha + \omega - \alpha' - \omega')(\alpha'\omega - \alpha\omega') + \alpha\alpha'(2(\alpha + \alpha') + 3(\omega + \omega')) + (\omega + \omega')(\alpha'\omega + \alpha\omega') + \alpha'^2\omega + \alpha^2\omega' \quad (19)$$

Like the velocity, the diffusion constant decreases as $\Delta\varepsilon$ increases in this regime. Note that the diffusion constant increases as $\Delta\mu$ increases, because $\Delta\mu$ enhances the rates of motion in both directions. In the limit $\Delta\mu/T \rightarrow \infty$ one obtains

$$D_{\max} = 2a_0^2 \frac{\omega\alpha' + \omega'\alpha + 2\alpha\alpha'}{\alpha + \alpha'}. \quad (20)$$

Again, for large chemical potential differences the result is independent of $\Delta\varepsilon$.

III. THE EFFECT OF HETEROGENEITY ON THE ENERGY LANDSCAPE

Next we discuss the effect of heterogeneity on the effective energy landscape experienced by motors or translocating polymers. The detailed dynamics which results will be considered in Sec. IV. As we shall see, heterogeneity has dramatic consequences over a range of parameters close to the stall force.

We first consider the somewhat simpler problem of heterogeneity and polymer translocation. We then show that a similar picture arises for motor proteins on heterogeneous substrates like DNA or RNA.

A. Polymer Translocation

Two sources of heterogeneity affect polymer translocation. Both arise for polymers composed of different types of monomer. We assume for simplicity that the monomers composing the polymer are drawn from some random distribution with a finite variance. Provided the correlations along the backbone are short range our results are insensitive to the exact nature of the distribution. The effect of sequence heterogeneity corresponding to a *particular* nucleotide sequence could easily be incorporated into a numerical analysis of the dynamics.

We first consider general features of the potential for a model with sequence heterogeneity. Randomness in the composition of the polymer will of course modify the interaction potential between the polymer and pore, $U(x)$. It is easy to see that this leads to a random potential component with a finite variance around its mean value, i.e., a random energy landscape. The second, more striking effect, arises from the randomness in the binding energy of the proteins. The associated force depends specifically on the location x along the polymer. In a convenient continuum notation, the total energy gained by attaching to the monomers

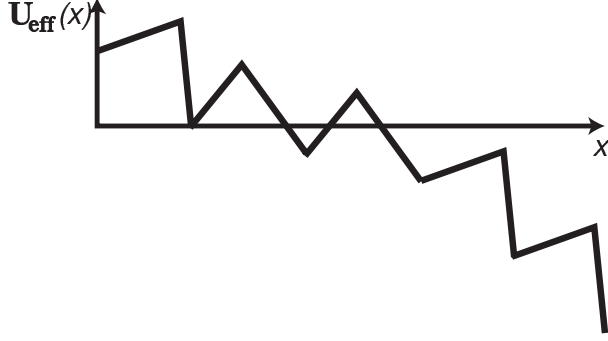


FIG. 8 Graphical representation of the energy landscape in the case of heterogeneous polymer translocation when the chemical environments on both sides of the pore are different. Potential fluctuations about the mean slope scale like \sqrt{x} for large x . The same picture holds for molecular motors moving on a heterogeneous substrate powered by a finite chemical potential difference.

has the form $\int_0^x F_\mu(x')dx'$, where $F_\mu(x)$ represents the different binding energies associated with the sequence of the polymer. If the sequence is random the fluctuations around the mean slope of the potential grow like \sqrt{x} . The effective potential experienced by the random walker is therefore

$$\mathbf{U}_{\text{eff}}(x) = U(x) - \left(\int_0^x F_\mu(x')dx' - Fx \right), \quad (21)$$

where we have included the externally applied force, F . A schematic representation of the potential is shown in Fig. 8. Since $\int_0^x F_\mu(x')dx'$ has fluctuations which grow as \sqrt{x} , the sequential binding of proteins to a translocating polymer creates a *random forcing* landscape, in contrast to the landscape defined by Eq. 1. Because the energy landscape itself can be viewed as a simple random walk about a linear landscape, the *random force* contribution to $\mathbf{U}_{\text{eff}}(x)$ (an integrated random walk) dominates the *random energy* term arising from interactions with the pore. As will be discussed in Section IV this results in unusual behavior if the externally applied force lies in a certain range of values near the stall force.

Note that it is also possible to obtain a purely random energy landscape in polymer translocation. When the chemical environments on both sides match (e.g., for identical concentrations of binding proteins) one has $F_\mu(x) = 0$. The only random component of the energy landscape is due to the potential for translocating through the pore which has bounded fluctuations about its mean value. For this energy landscape, the dynamics at long times and large length scales is then biased diffusion, with a drift velocity and diffusion constant renormalized by the heterogeneous interactions with the pore (Alexander et al.,

1981).

We now explore these effects within our microscopic model of polymer translocation. The heterogeneity is introduced into the model through the rates (2). Imagine drawing the set of parameters $\{p\} = \{\omega, \omega', \Delta\varepsilon, \Delta\mu\}$ from random distributions (corresponding to various nucleotide sequences) with a finite variance. According to Eq. (5), the total change in energy after m monomers translocate is given by

$$E(m) = 2fm + \sum_{l=1}^m \Delta E(l) . \quad (22)$$

Here the $\Delta E(m)$ are effective energy differences between two even sites corresponding to the set of values of the set $\{p\}$ drawn randomly. Since the energy is a sum of independent random variables a *random forcing* landscape is developed.

We expect that a simple *random energy* landscape results if we turn off the protein binding by setting $\Delta\mu = 0$. However, because the energy at even sites is always $E = 0$ in our simple model, the landscape is just a uniform tilt in this limit. A more realistic model would allow additional energy variations at these sites. If we assign an energy $\varepsilon(m)$ to these even sites, it is straightforward to show that the total change in energy after m monomers have translocated takes the form

$$E(m) = 2fm + \varepsilon(m) , \quad (23)$$

corresponding to a random energy landscape.

B. Molecular Motors

We now turn to the effect of heterogeneity on molecular motors. Here, as for polymer translocation, we select the set of parameters $\{p\} = \{\alpha, \alpha', \omega, \omega', \Delta\varepsilon\}$ from a random distribution with a finite variance. For some motors and enzymes (for example RNA Polymerase, helicases, DNA polymerases and exonucleases – see introduction and below), $\Delta\mu$ may also be random. This clearly only adds an additional contribution to the random forcing landscape. Using the results presented above it is easy to see from Eq. (15) that the total effective energy change after m monomers is given by

$$E(m) = 2fm + \sum_{l=1}^m \Delta E(l) . \quad (24)$$

Here, each $\Delta E(m)$ corresponds to an independent set of values of $\{p\}$ drawn randomly. Thus, as in the polymer translocation problem, the potential is random forcing.

For motors such as helicases, DNA polymerase and exonucleases, and RNA polymerase and ribosomes an additional contribution to the random energy arises due to the force associated with, e.g., base pairing energies or the trailing strand which is produced. The effect of this would be to modify the expression above to

$$E(m) = 2fm + \sum_{l=1}^m f_{\mu}(l) + \sum_{l=1}^m \Delta E(l) , \quad (25)$$

where f_{μ} is the additional contribution of the explicit random forcing from monomer m . The resulting random forcing landscape is even more pronounced.

The above scenario applies as long as the chemical potential difference $\Delta\mu \neq 0$. In the case when $\Delta\mu = 0$ it is easy to see that $\Delta E(m) = 0$ unless we allow, as in the polymer translocation problem, for the energy at even sites also to vary and take the value $\varepsilon(m)$. In this case we obtain

$$E(m) = 2fm + \varepsilon(m) , \quad (26)$$

corresponding to a random energy landscape provided $\varepsilon(m)$ has only short range correlations. Although we could write the energy in the form of Eq. 24, now $\Delta E(m) = \varepsilon(m) - \varepsilon(m-1)$, so $\Delta E(m)$ is effectively the gradient of a random potential with bounded fluctuations. Note, however, that for motors with an f_{μ} contribution (as in Eq. (25)) it is not possible to obtain a random energy landscape.

The energy landscape for both polymer translocation and molecular motors is therefore qualitatively identical. Generically, in both cases, a random forcing energy landscape develops. However, if the motor model without the applied external force has no bias (i.e., if $\Delta\mu = 0$), we recover the diffusion with drift dynamics associated with a random energy potential.

IV. DYNAMICS IN HETEROGENEOUS ENVIRONMENTS

In this section we discuss in detail the dynamics of translocating polymers and motor proteins with heterogeneity for the model depicted schematically in Fig. 6. We describe four distinct cases with different dynamical behaviors as the externally applied force is varied. The critical forces for the transition between the regimes can be calculated exactly

in terms of the rates $w_a^\rightarrow, w_b^\leftarrow, w_a^\leftarrow, w_b^\rightarrow$ averaged over their heterogeneous generalization with $f = 0$. The explicit expressions for polymer translocation and molecular motors can be easily obtained by using the rates in Eqs. (2) and (13) respectively. We assume throughout that $\Delta\mu \neq 0$, as the case $\Delta\mu = 0$ leads only to a random energy model and biased diffusion. Also, contributions to the random forcing energy landscape of the form of Eq. (25) are omitted for simplicity. Their addition is straightforward and can be easily seen to enhance the region of anomalous dynamics.

The dynamical behaviors of random walkers in random forcing or random energy landscapes have been studied in detail in the statistical mechanics literature (Bouchaud et al., 1990; Derrida, 1983). Unusual dynamical behavior arises for random walkers in a random forcing energy landscape. Using the results of Derrida (Derrida, 1983), one can calculate the transition points between the different regimes including the effect of randomness. Parts of the calculation are outlined in Appendix C along with the different regimes in terms of the transition rates $w_a^\rightarrow, w_b^\leftarrow, w_a^\leftarrow, w_b^\rightarrow$. Here we consider the experimental setup in Figs. 4 and 6 where the external force is varied. Denoting spatial averages by an overline and using the results of the Appendix C one finds the following regimes.

Regime I: The velocity v and diffusion constant D of the model are finite when

$$f < -\frac{T}{4} \ln \left(\overline{\left(\frac{w_a^\leftarrow w_b^\leftarrow}{w_a^\rightarrow w_b^\rightarrow} \right)^2} \right)_{f=0}, \quad (27)$$

or

$$f > \frac{T}{4} \ln \left(\overline{\left(\frac{w_a^\rightarrow w_b^\rightarrow}{w_a^\leftarrow w_b^\leftarrow} \right)^2} \right)_{f=0}, \quad (28)$$

where the subscript $f = 0$ denotes that f has been set to zero in the average. In this regime $\langle x \rangle = vt$ and $\langle x^2 \rangle - \langle x \rangle^2 = 2Dt$ for long times, where the angular brackets denote an average over different thermal histories of the system. Simpler conditions can be obtained by assuming that $\Delta E(m) = T \ln((w_a^\leftarrow w_b^\leftarrow)/(w_a^\rightarrow w_b^\rightarrow))$ has a *Gaussian* distribution about the mean $2f + \overline{\Delta E}_{f=0}$ (see Eqs. 5 and 15) and a variance $V = \overline{(\Delta E)^2}_{f=0} - (\overline{\Delta E})_{f=0}^2$. Here again the subscript $f = 0$ denotes that averages are taken with the value of the force set to zero. In the case one has

$$\begin{aligned} f &> \frac{1}{2} \left(\overline{\Delta E}_{f=0} + V/T \right), \\ f &< \frac{1}{2} \left(\overline{\Delta E}_{f=0} - V/T \right). \end{aligned} \quad (29)$$

Note that the force does not contribute to the variance so that $V = \overline{\Delta E^2}_{f=0} - \overline{\Delta E}_{f=0}^2 = \overline{\Delta E_f^2} - \overline{\Delta E_f}^2$.

Regime II: The velocity v is finite but the diffusion constant is infinite. Thus, in this region $\langle x \rangle = vt$ and $\langle x^2 \rangle - \langle x \rangle^2 \sim t^{2/\mu}$, where $1 < \mu < 2$. The relevant force ranges are

$$-\frac{T}{4} \ln \left(\frac{\overline{w_a^{\leftarrow} w_b^{\leftarrow}}}{\overline{w_a^{\rightarrow} w_b^{\rightarrow}}} \right)_{f=0} < f \leq -\frac{T}{2} \ln \left(\frac{\overline{w_a^{\leftarrow} w_b^{\leftarrow}}}{\overline{w_a^{\rightarrow} w_b^{\rightarrow}}} \right)_{f=0}, \quad (30)$$

and

$$\frac{T}{2} \ln \left(\frac{\overline{w_a^{\rightarrow} w_b^{\rightarrow}}}{\overline{w_a^{\leftarrow} w_b^{\leftarrow}}} \right)_{f=0} \leq f < \frac{T}{4} \ln \left(\frac{\overline{w_a^{\rightarrow} w_b^{\rightarrow}}}{\overline{w_a^{\leftarrow} w_b^{\leftarrow}}} \right)_{f=0}^2. \quad (31)$$

Provided that ΔE has a Gaussian distribution the conditions reduce to

$$\begin{aligned} \frac{1}{2} (\overline{\Delta E}_{f=0} + V/2T) < f \leq \frac{1}{2} (\overline{\Delta E}_{f=0} + V/T), \\ \frac{1}{2} (\overline{\Delta E}_{f=0} - V/T) \leq f < \frac{1}{2} (\overline{\Delta E}_{f=0} - V/2T). \end{aligned} \quad (32)$$

For a Gaussian distribution it is known (Bouchaud et al., 1990) that the exponent μ is given by

$$\mu = 2T |\overline{\Delta E}_{f=0} - 2f| / V. \quad (33)$$

Regime III: The velocity v is zero in the sense that $\langle x \rangle \sim t^\mu$, where $\mu < 1$. The exponent μ also controls the variance, $\langle x^2 \rangle - \langle x \rangle^2 \sim t^{2\mu}$. This behavior occurs when

$$-\frac{T}{2} \ln \left(\frac{\overline{w_a^{\leftarrow} w_b^{\leftarrow}}}{\overline{w_a^{\rightarrow} w_b^{\rightarrow}}} \right)_{f=0} \leq f \leq \frac{T}{2} \ln \left(\frac{\overline{w_a^{\rightarrow} w_b^{\rightarrow}}}{\overline{w_a^{\leftarrow} w_b^{\leftarrow}}} \right)_{f=0}. \quad (34)$$

When ΔE has a Gaussian distribution, these conditions reduce to

$$\frac{1}{2} (\overline{\Delta E}_{f=0} - V/2T) < f < \frac{1}{2} (\overline{\Delta E}_{f=0} + V/2T). \quad (35)$$

Sinai diffusion: Here $\langle x \rangle = 0$ and $\langle x^2 \rangle \sim (\ln(t/\tau))^4$, where τ is the microscopic time needed to move across one monomer. This regime appears precisely at the ‘‘stall force’’ corresponding to a disordered substrate, namely

$$f_s = \frac{T}{2} \ln \left(\frac{\overline{w_a^{\rightarrow} w_b^{\rightarrow}}}{\overline{w_a^{\leftarrow} w_b^{\leftarrow}}} \right)_{f=0}. \quad (36)$$

If ΔE has a Gaussian distribution this condition yields

$$f_s = \frac{\overline{\Delta E}_{f=0}}{2}. \quad (37)$$

The resulting behavior as the force is varied is summarized qualitatively in Fig. 1.

It is interesting to consider the location of the stall force, f_s , as well as the range of forces over which the displacement is anomalous, namely the region where $v = \lim_{t \rightarrow \infty} \langle x \rangle / t = 0$, in some more detail for both polymer translocation and molecular motors in some simple scenarios. These quantities characterize how the location and width of the anomalous displacement region develops as a function of temperature and chemical forces. We assume $\Delta E(m)$ with a Gaussian distribution about $\overline{\Delta E}$ with a variance V , although it is straight forward to extend the results to non-Gaussian distributions with no change of the qualitative behavior. It is straightforward to show using Eq. (35) that the range of forces, Δf , over which the velocity is zero satisfies

$$\Delta f = \frac{1}{2T} V. \quad (38)$$

For polymer translocation using Eqs. (5) and 37 implies that Sinai diffusion occurs for the force

$$f_s = \frac{\overline{\Delta \mu}}{2}, \quad (39)$$

while Eq. 38 implies that the range of forces around f_s where the displacement is anomalous is given by

$$\Delta f = \frac{1}{2T} (\overline{\Delta \mu^2} - \overline{\Delta \mu}^2). \quad (40)$$

If there are no proteins on lefthand side (cis chamber) and a small concentration, P , of protein is added to the righthand side (trans chamber) one can show using (A3) that $f_s \propto P$ while $\Delta f \propto P^2$. Thus, as the chemical bias increases both f_s and Δf grow. Note that in general one may consider proteins in both the left and right chambers. In this case even when the average chemical bias $\overline{\Delta \mu} = 0$ one may still have $V > 0$ giving rise to anomalous dynamics even when the external bias $F = 0$.

For molecular motors the situation is more interesting. The results presented above for the transition points between the different regimes hold even when $\Delta \mu$ is also random. However, here we restrict ourselves to the simpler case when $\Delta \mu$ is constant. In this case (15) implies that for small chemical potential ($\Delta \mu / T \ll 1$) the chemical energy difference $\Delta E_{f=0} = q \Delta \mu$, where q is the coefficient in the Taylor expansion of (15) in $\Delta \mu$ which is independent of T . Therefore, in this limit, the stall force is

$$f_s = \frac{\bar{q} \Delta \mu}{2}, \quad (41)$$

and

$$\Delta f = \frac{\Delta\mu^2}{T} (\overline{q^2} - \overline{q}^2) , \quad (42)$$

where we have assumed the purpose of a rough estimate that the chemical potential difference does not depend on the type of monomer. Similarly to polymer translocation, as the system is driven out of chemical equilibrium both f_s and Δf grow. However, in the limit of $\Delta\mu/T \gg 1$ one obtains $\Delta E_{f=0} = pT$ where p is obtained by taking the appropriate limit in (15) and is independent of T . We then have

$$f_s = \frac{\overline{p}T}{2} , \quad (43)$$

and

$$\Delta f = T (\overline{p^2} - \overline{p}^2) , \quad (44)$$

implying that both quantities *increase* with increasing temperature.

Note that if the force applied to the polymer or motor is held constant and the chemical parameters (e.g. ATP or protein concentration) are varied from their equilibrium value one should also observe a region of anomalous displacement (see the general expressions in Appendix C). These conclusions are summarized qualitatively in Figs. 1, 2 and 3.

V. EXPERIMENTAL CONSIDERATIONS

As discussed in the previous section, the important quantity for deciding if anomalous dynamics is present is the variance $V \equiv \overline{(\Delta E)^2} - (\overline{\Delta E})^2$ of $\Delta E(m)$, where the overbar represents an average over the ensemble of random sequences. Effects related to sequence heterogeneity dominate when V is large compared to $k_B T \overline{\Delta E}$. Here we estimate the ranges over which anomalous dynamics may be observed in experiments as well as other preconditions needed to observe this behavior. We also discuss the effect of finite time experiments on the shape of the velocity-force curve. In this section, we reintroduce Boltzmann's constant k_B .

A. Polymer Translocation

For polymer translocation, whether the variance V is large compared to $k_B T \overline{\Delta E}$ of course depends on a number of factors, including the base composition of the polynucleotide passing

through the pore, the particular protein whose binding drives translocation, and the concentration of the binding protein. Nonetheless, it is instructive to consider an example to get some sense of the orders of magnitude involved. We focus on DNA binding proteins. Note that, like those of most such proteins, the binding sites are several nucleotides long; unlike in previous sections, unless stated otherwise, we will give values of V and other parameters normalized per nucleotide rather than per bound protein.

The bacteriophage T4-coded gene 32 protein (gp32) is a monomeric single-stranded DNA (ssDNA) binding protein which is implicated in DNA replication and related processes (Colman and Oakley, 1980). When it associates with ssDNA cooperatively in the “polynucleotide” mode (Kowalczykowski et al., 1981), its net affinity¹ K_{net} can vary by as much as a factor of 10 depending on the polymer’s base composition; in physiological salt concentrations, a typical range is $K_{\text{net}} \sim 2 \times 10^8 - 2 \times 10^9 \text{ M}^{-1}$ (Newport et al., 1981). In this binding mode, the binding site of each gp32 monomer is 7 nucleotides long. For a μM protein concentration, K_{net} is large enough that almost all sites on the translocated ssDNA will be occupied. Upon assuming that V is determined entirely by the base dependence of K_{net} , we then estimate that $V \sim 0.1 - 0.2(k_B T)^2$ for a “generic” DNA molecule in which each of the bases appears with roughly equal frequency. Here T is room temperature, $k_B T \simeq 0.59 \text{ kcal/mole}$. In this case, the change in free energy of a nucleotide moved from a buffer without any gp32 to one where the protein is present is $\Delta\mu \sim k_B T$ (see Eq. 2). Upon taking the ssDNA to be a freely-jointed chain with Kuhn length 1.5 nm (Smith et al., 1996), one finds that a force of about 10–15 pN on the polymer is required to cancel the effects of the protein binding. In order to have $k_B T \overline{\Delta E} \lesssim V$, so that disorder effects can be detected, the value of the force must be controlled to roughly 10% or better accuracy.

B. Molecular Motors

To be able to measure the motion of a motor along a substrate it must remain attached long enough to be able to preform many moves across monomers. In other words, if the rate at which the motor leaves the substrate is γ and the rate of crossing a monomer to the right

¹ The net affinity is the affinity of an additional protein molecule for a growing chain of cooperatively bound monomers; it differs from the affinity of an isolated protein molecule for ssDNA by an enhancement factor arising from the cooperative interactions

or left is w^{\rightarrow} or w^{\leftarrow} respectively, then $\gamma \ll w^{\rightarrow} + w^{\leftarrow}$ must hold. In the regime of anomalous dynamics w^{\rightarrow} is of the same order of w^{\leftarrow} . Therefore, the condition will not be fulfilled in this regime when the rate of hopping against the chemical bias w^{\leftarrow} is always very small.

There are, however, experiments where such a restriction does not hold. For example, the experiment by Wuite et al. (Wuite et al., 2000) on the DNA polymerase/exonuclease system (see also (Maier et al., 2000)) monitors not the displacement of a single motor but the location of the *junction* between the ssDNA and the dsDNA. Therefore, it is more natural to model the dynamics of the ssDNA/dsDNA junction and not of the motor. A motor which leaves the ssDNA/dsDNA junction is eventually replaced by a motor from the solution. Within our models this can be represented by an internal state of the junction (similar in spirit to (Fisher and Kolomeisky, 1999) and (Kolomeisky and Fisher, 1999)). A model of this type for the DNA polymerase/exonuclease has been studied in (Goel et al., 2003). However, the disorder in the transition rates, present due to the heterogeneity of the DNA, has been neglected. In Appendix D we analyze in some detail a simple model of the DNA polymerase/exonuclease system. As shown in the appendix it is straight forward to show that the presence of heterogeneity (for example, in the energy gained from the hydrolysis of the different NTP's) leads to a random forcing energy landscape. One therefore expects a region of anomalous dynamics near where the external stretching force F' causes a change in direction. We stress that more realistic models with many intermediate states can be analyzed similarly without affecting the existence of the region with anomalous dynamics. Unfortunately, for this experiment an estimation of the width of the region is not straightforward.

Estimates, similar to those above for polymer translocation, can be obtained for the random force landscapes for a number of molecular motors which operate on DNA or RNA. Two examples of interest are RNA polymerases (RNAP's) (Davenport et al., 2000; Gelles and Landick, 1998; Jülicher and Bruinsma, 1998; Wang et al., 1998) and helicases acting on double-stranded DNA (dsDNA) (Bianco et al., 2001; Dohoney and Gelles, 2001; Lohman and Bjornson, 1996; von Hippel and Delagouette, 2001). An RNAP's function is to transcribe DNA—that is, to synthesize an RNA “copy” with the same sequence as a DNA molecule. To do so, it walks along dsDNA trailing a growing RNA strand. The RNAP motor is powered entirely by the energy gained from the hydrolysis of successive nucleotide triphosphates (NTP's) as they are added to the RNA molecule. Although the mechanism of RNAP

motion is still the subject of debate (Jülicher and Bruinsma, 1998; von Hippel and Pasmán, 2002), many models suggest that at low enough NTP concentrations, its ability to move forward will be limited by the rate at which NTP’s arrive at the catalytic site. A straightforward way to force RNAP into a regime in which its motion is dominated by a random force energy landscape is thus to place it in a buffer with different concentrations of each of the four NTP’s. The motor’s ability to take a forward step is dependent on the incorporation of the appropriate NTP, and the rate of that incorporation is proportional to that NTP’s concentration. Thus, one can in principle make V arbitrarily large and satisfy the criterion $V > k_b T \overline{\Delta E}$ for significant random force effects. Each factor of 10 difference between the concentrations of two nucleotide triphosphates, and hence in the rates to make a forward step, translates into a difference of $k_B T \ln(10) \approx 2.3 k_B T$ in $\Delta E(m)$. Of course, in practice other factors—for example the possibility that the RNAP might fall off its DNA track before the needed NTP arrives—will limit how large a range of concentration differences can be achieved experimentally. It will be interesting to see whether strong disorder effects can be observed.

Another class of motors that use DNA as their track are helicases, which are needed to separate the two strands of dsDNA in order to facilitate various processes in the cell such as cell division in prokaryotes. Helicases move along the DNA by consuming energy from NTP’s. While some helicases only break a few base pairs at a time, others can move substantial distances along their tracks (Bianco et al., 2001; Dohoney and Gelles, 2001). Recent modelling of certain monomeric helicases (Betterton and Jülicher, 2003) suggests that disordered DNA sequences affect helicase motion primarily through the different energies required to open different base pairs. Random sequences thus lead to anomalous helicase motion in much the same way they do anomalous dynamics of mechanical unzipping (Lubensky and Nelson, 2000, 2002). In the simplest case of “passive” opening, one finds that $\Delta E(m) \approx \Delta E_{\text{motor}} + \Delta E_{\text{DNA}}(m)$, where ΔE_{motor} , which summarizes the forward force exerted by the helicase motor, is negative and has magnitude at least $\sim 2k_B T$, and ΔE_{DNA} is simply the thermodynamic free energy cost of opening each successive base pair, with size roughly between 1 and 3 kT (SantaLucia, 1998). One thus has $V \sim 1(k_B T)^2$. This large variance means that it should be relatively easy to observe anomalous, disorder-dominated dynamics in helicases as predicted earlier for DNA unzipping. If, for example, one assumes that the magnitude of ΔE_{motor} is near its lower bound of $2k_B T$, then, in the passive opening

model, disorder effects should begin to appear for a mechanical load opposing the motor's motion of as little as 7 pN and should persist up to at least 20 pN.

C. Finite time effects

All calculations of quantities such as the velocity have been done by taking the limit of very large times and averaging over thermal realizations with the same heterogeneous sequence. For experiments done over finite times the velocity will not be strictly zero in the regime of anomalous dynamics. Instead, the velocity decays to zero as $t_E^{\mu-1}$, where t_E is the experimental averaging time used to define v as $\langle x(t_E) - x(0) \rangle / t_E$. The closer μ is to zero, the faster the decay will be. Therefore, the curve of the velocity as a function of the external force or chemical potential (see Figs. 1 and 2) will be rounded becoming sharper and sharper as $t_E \rightarrow \infty$. To illustrate this we have carried out simulations of model (13) on a single realization of the disorder averaging over thermal realizations and measured the $v - F$ curve. The results are shown in Fig. 9. As can be seen the longer t_E the closer is the $v - F$ curve to that shown in Fig. 1. The convex shape of the curve near the stall force is clear already for averaging times $t_E \sim 10^5$, corresponding to motors which transverse distances of $O(1000)$ at $f/T = 0$. Note that, if one looks at the displacement of a single motor (i.e., without averaging over thermal realizations), the regime of anomalous dynamics will be characterized by long pauses at localized regions (corresponding to deep minima of the effective potential) with fast transitions between the localized regions (corresponding to overcoming the barrier associated with the minima). The inset of Fig. 9 shows a single trajectory of as a function of time for a given realization of disorder. The value of f/T was chosen to be in the region close to the anomalous velocity regime but not inside it (the point is at the edge of the anomalous diffusion region close to the normal diffusion region). As can be seen the motion of the motor is characterized by long pauses at specific locations along the track, with quick jumps between the pause points. The location of the pause points is reproducible for the same spatial disorder and different thermal realizations although their duration varies from simulation to simulation. Note, that since the velocity is finite in this regimes, over large length scales the effect of the jumps becomes unimportant. These pauses correspond to local minima of the effective potential and as such are inherently correlated with the structure of the track. Such pauses and jumps have been observed in

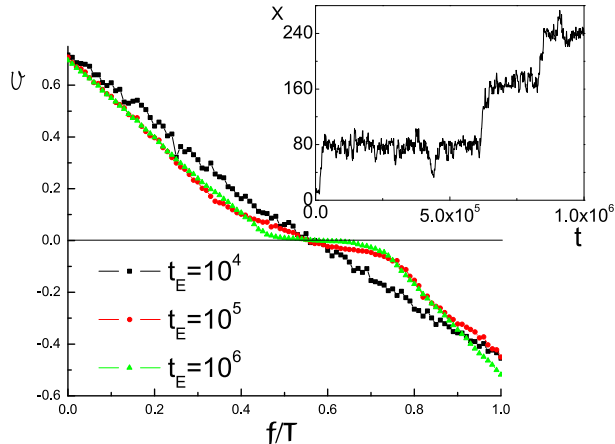


FIG. 9 The velocity as a function of f/T for different values of t_E . Here $\Delta\mu/T = 3$ and parameters were chosen with equal probability to be either $\{p\} = \{5, 1, 0.3, 1, 0\}$ or $\{p\} = \{4, 0.1, 0.7, 1, 0\}$ (see text for notation). The calculated regime of anomalous velocity is $0.5116 < f < 0.699$. Data was averaged over a 100 thermal realizations. Inset: a single trajectory shown for the same parameters at $f/T = 0.45$.

recent experiments (Danilowicz et al., 2003) on DNA unzipping.

VI. SUMMARY

We have studied the effect of sequence heterogeneity on both polymer translocation and the motion of molecular motors within simple models. The models were solved exactly both with and without disorder. It was shown that these systems can be represented on large length scales and long times by a random walker moving along a random forcing energy landscape. Thus, in a range of forces near the stall force we expect anomalous dynamics where the displacement grows as a sublinear power of time. We stress again that such results also apply to more sophisticated models which include many internal states of the motor (see the discussion of the DNA polymerase / exonuclease system in Appendix D). Several systems in which the regime of anomalous dynamics might be wide enough to be observable were considered.

Acknowledgments: It is a pleasure to acknowledge helpful conversations with S. Block, A. Meller and S. Xie. We are grateful to A. Goel for a copy of (Goel et al., 2003) prior to publication and to G. Lattanzi and A. Maritan for pointing out a misprint. Work by Y.K and D.R.N was supported by the National Science Foundation through Grant DMR-0231631

and the Harvard Materials Research Laboratory via Grant DMR-0213805. Y.K also thanks the Fulbright program in Israel for financial support.

APPENDIX A: The chemical potential difference for translocating polymers

Here we discuss the dependence of the chemical potential difference $\Delta\mu$ for a translocating polymer between the righthand (trans) and lefthand (cis) sides of Fig. 4 on the protein concentrations and its binding energy to the polymer. Consider first a denatured polymer in a solution with a concentration c_p of proteins which can bind to its monomers with a binding energy $E_b < 0$. We neglect cooperativity in the binding of the proteins to the polymer, although this effect could easily be included. Assuming an ideal solution theory the protein chemical potential is given $\mu = \mu_0 + T \ln(P)$, where $P = c_p/c$ and c is the concentration of the solvent. Here we take the free-energy change due to an addition of one isolated protein to the solvent to be $\mu_0 - T \ln n$ where n is the number of solvent molecules (Landau and Lifshitz, 1963). Next, we take the energy function of a polymer of length N inside the solution to be

$$H = \sum_{i=1}^N (-E_b \sigma_i + \mu' \sigma_i) , \quad (\text{A1})$$

where $\sigma_i = 1(0)$ if a protein is bound (unbound) to monomer i and μ' is a chemical potential which controls the density of proteins bound to the polymer. In thermal equilibrium $\mu = \mu'$ which gives for the free energy of a polymer monomer in the solution

$$- T \ln (1 + P \exp(\mu_0 - E_b)/T)) . \quad (\text{A2})$$

The change in the free energy of the polymer which occurs as a result of a monomer passing from the left (cis) chamber to the right (trans) chamber, with ratios of protein to solvent concentrations P_L and P_R respectively, is given by

$$\Delta\mu = \frac{d\mathcal{F}}{dN_R} = -T \ln \left(\frac{1 + P_L \exp(\mu_0 - E_b)/T)}{1 + P_R \exp(\mu_0 - E_b)/T)} \right) . \quad (\text{A3})$$

where \mathcal{F} is the total free energy of the polymer and N_R is the number of monomers in the right chamber. It is straightforward to see that this result implies that for proteins with different binding energy to different types of monomers $\Delta\mu$ will depend on the type of monomer.

APPENDIX B: Deriving the effective potential from the master equation

In this appendix we show that the equations for the probability $P_n(t)$ of being at site n at time t are equivalent in the long-time limit (to be specified more exactly below) to a random walker moving in an energy landscape constructed using Eq. (4). We demonstrate this by eliminating the even sites from the equations of motion (see (Lattanzi and Maritan, 2002) for similar ideas).

First, consider the equations governing the evolution of the probability, i.e. the master equation. For odd n one has (see Fig. 6)

$$\frac{dP_n(t)}{dt} = w_a^{\rightarrow} P_{n-1}(t) + w_a^{\leftarrow} P_{n+1}(t) - (w_b^{\rightarrow} + w_b^{\leftarrow}) P_n(t) , \quad (\text{B1})$$

while for even n

$$\frac{dP_n(t)}{dt} = w_b^{\rightarrow} P_{n-1}(t) + w_b^{\leftarrow} P_{n+1}(t) - (w_a^{\rightarrow} + w_a^{\leftarrow}) P_n(t) . \quad (\text{B2})$$

Next, we solve the equation for the odd sites and substitute into that for the even sites. The solution of the equation for the odd sites is

$$P_n(t) = e^{-(w_b^{\rightarrow} + w_b^{\leftarrow})t} \left(P_n(0) + \int_0^t d\tau e^{(w_b^{\rightarrow} + w_b^{\leftarrow})\tau} (w_a^{\rightarrow} P_{n-1}(\tau) + w_a^{\leftarrow} P_{n+1}(\tau)) \right) , \quad (\text{B3})$$

where $P_n(0)$ is the probability distribution at the initial time $t = 0$. Substituting this into the equation for the even sites yields

$$\begin{aligned} \frac{dP_n(t)}{dt} &= e^{-(w_b^{\rightarrow} + w_b^{\leftarrow})t} \int_0^t d\tau e^{(w_b^{\rightarrow} + w_b^{\leftarrow})\tau} (w_b^{\rightarrow} w_a^{\rightarrow} P_{n-2}(\tau) + w_b^{\leftarrow} w_a^{\leftarrow} P_{n+2}(\tau)) \\ &+ e^{-(w_b^{\rightarrow} + w_b^{\leftarrow})t} \int_0^t d\tau e^{(w_b^{\rightarrow} + w_b^{\leftarrow})\tau} (w_b^{\rightarrow} w_a^{\leftarrow} + w_b^{\leftarrow} w_a^{\rightarrow}) P_n(\tau) \\ &- (w_a^{\rightarrow} + w_a^{\leftarrow}) P_n(t) + e^{-(w_b^{\rightarrow} + w_b^{\leftarrow})t} (w_b^{\rightarrow} P_{n-1}(0) + w_b^{\leftarrow} P_{n+1}(0)) . \end{aligned} \quad (\text{B4})$$

At times $t \gg (w_b^{\rightarrow} + w_b^{\leftarrow})^{-1}$ one can neglect the two last terms in (B4) and approximate the integrals as follows

$$\int_0^t d\tau e^{(w_b^{\rightarrow} + w_b^{\leftarrow})\tau} f(\tau) \approx \frac{1}{(w_b^{\rightarrow} + w_b^{\leftarrow})} e^{(w_b^{\rightarrow} + w_b^{\leftarrow})t} f(t) \quad (\text{B5})$$

where $f(\tau)$ is assumed to vary slowly with τ . In this long time approximation, Eq. (B4) reduces to

This reduces (B4) to

$$\frac{dP_n(t)}{dt} = w_b^{\leftarrow} w_a^{\leftarrow} P_{n+2}(t) + w_b^{\rightarrow} w_a^{\rightarrow} P_{n-2}(t) - (w_b^{\rightarrow} w_a^{\rightarrow} + w_b^{\leftarrow} w_a^{\leftarrow}) P_n(t) \quad (\text{B6})$$

where we have rescaled times such that $t \rightarrow \frac{t}{(w_b^{\rightarrow} + w_b^{\leftarrow})}$. As expected this equation corresponds to a random walker moving in a potential constructed using Eq. (4).

APPENDIX C: Derivation of the Different Dynamical Regimes

In this appendix the expressions for the different dynamical regimes in terms of the hopping rates $w_a^\rightarrow, w_a^\leftarrow, w_b^\rightarrow, w_b^\leftarrow$ are given. These general equations allow a straightforward derivation of the expressions in the text. However, before turning to the results we outline the derivation of the regime where the displacement is anomalous. The derivation of the other regimes is much lengthier, so we only sketch the main results.

Unless stated otherwise we assume throughout this appendix that

$$\overline{\log\left(\frac{w_a^\leftarrow w_b^\leftarrow}{w_a^\rightarrow w_b^\rightarrow}\right)} < 0, \quad (\text{C1})$$

where, as in the main text, we denote spatial averages by an overbar. Because $\exp(-\Delta E/T) = w_a^\leftarrow w_b^\leftarrow / w_a^\rightarrow w_b^\rightarrow$ in our notation, this condition is equivalent to assuming an overall bias to the right

$$\overline{\Delta E} < 0, \quad (\text{C2})$$

where ΔE arises from the generalization of Eqs. (5) and (15) to heterogeneous systems. The other opposite regime $\overline{\Delta E} > 0$ can be treated similarly. As shown by Derrida (Derrida, 1983) the velocity of a random walker on an infinite lattice model in this case is given by

$$v = \lim_{N \rightarrow \infty} \frac{N}{\sum_{i=1}^N r_i}, \quad (\text{C3})$$

where

$$r_i = \frac{1}{W_{i+1,i}} \left[1 + \sum_{k=1}^{N-1} \prod_{l=1}^k \left(\frac{W_{i+l-1,i+l}}{W_{i+l+1,i+l}} \right) \right]. \quad (\text{C4})$$

Here $W_{i,j}$ is the hopping rate from site j to i . The denominator of (C3) can be simplified by replacing the sum by an average of r_i

$$\langle r \rangle = \lim_{N \rightarrow \infty} \frac{1}{N} \sum_{i=1}^N r_i. \quad (\text{C5})$$

Using the rates $w_a^\rightarrow, w_a^\leftarrow, w_b^\rightarrow, w_b^\leftarrow$ one finds that the average $\langle r \rangle$ is finite only if

$$\overline{\left(\frac{w_a^\leftarrow w_b^\leftarrow}{w_a^\rightarrow w_b^\rightarrow}\right)} < 1. \quad (\text{C6})$$

In this case the velocity is finite. However, when the inequality is reversed $\langle r \rangle = \infty$ and the velocity is zero.

A much lengthier calculation along somewhat similar lines can be done to derive the other dynamical regimes. One obtains the following results.

Regime I: When

$$\overline{\left(\frac{w_a^{\leftarrow} w_b^{\leftarrow}}{w_a^{\rightarrow} w_b^{\rightarrow}}\right)^2} < 1, \quad (\text{C7})$$

the velocity v and diffusion constant D of the model are finite. Namely, $\langle x \rangle = vt$ and $\langle x^2 \rangle - \langle x \rangle^2 = 2Dt$ for long times, where the angular brackets denote an average over different thermal histories of the system. Assuming for simplicity that $\Delta E(m)$ is distributed around $\overline{\Delta E}$ with a Gaussian distribution with a variance $V = \overline{(\Delta E)^2} - (\overline{\Delta E})^2$ this condition reduces to

$$\frac{T|\overline{\Delta E}|}{V} > 1, \quad (\text{C8})$$

i.e. the variance of the energy fluctuations must not be too large. Here we have used the fact that $\overline{\Delta E} < 0$ and the relation $\overline{e^x} = e^{\overline{x} + (\overline{x^2} - \overline{x}^2)/2}$ which holds for Gaussian distributions.

Regime II: When

$$\overline{\left(\frac{w_a^{\leftarrow} w_b^{\leftarrow}}{w_a^{\rightarrow} w_b^{\rightarrow}}\right)} < 1 \leq \overline{\left(\frac{w_a^{\leftarrow} w_b^{\leftarrow}}{w_a^{\rightarrow} w_b^{\rightarrow}}\right)^2}, \quad (\text{C9})$$

the velocity v is finite but the diffusion constant is infinite. It can be shown (Bouchaud et al., 1990) that in this region the long time behavior is $\langle x \rangle = vt$ and $\langle x^2 \rangle - \langle x \rangle^2 \sim t^{2/\mu}$, where $1 < \mu < 2$. If we assume a mean value of ΔE with a Gaussian distribution about the mean, the condition reduces to

$$1/2 < \frac{T|\overline{\Delta E}|}{V} \leq 1. \quad (\text{C10})$$

We have again used $\overline{\Delta E} < 0$. For this case it is known (Bouchaud et al., 1990) that the exponent μ is given by $\mu = 2T|\overline{\Delta E}|/V$.

Regime III: When

$$\overline{\left(\frac{w_a^{\leftarrow} w_b^{\leftarrow}}{w_a^{\rightarrow} w_b^{\rightarrow}}\right)} > 1, \quad (\text{C11})$$

the velocity v is zero. More precisely $\langle x \rangle \sim t^\mu$ where $\mu < 1$. The diffusion about this drift is anomalous in the sense that $\langle x^2 \rangle - \langle x \rangle^2 \sim t^{2\mu}$. Assuming again a mean value of ΔE with a Gaussian distribution about the mean leads to the condition

$$\frac{T|\overline{\Delta E}|}{V} \leq 1/2, \quad (\text{C12})$$

where again we have used the fact that $\overline{\Delta E} < 0$.

Sinai diffusion: When the average bias is exactly zero,

$$\overline{\log\left(\frac{w_a^{\leftarrow} w_b^{\leftarrow}}{w_a^{\rightarrow} w_b^{\rightarrow}}\right)} = 0, \quad (\text{C13})$$

the system exhibits Sinai diffusion (Sinai, 1982) with $\langle x \rangle = 0$ and $\langle x^2 \rangle \sim (\ln(t/\tau))^4$, where τ is the microscopic time needed to move one monomer. Thus, we are now considering the case $\overline{\Delta E} = 0$.

Note that when

$$\overline{\log \left(\frac{w_a^\leftarrow w_b^\leftarrow}{w_a^\rightarrow w_b^\rightarrow} \right)} > 0, \quad (\text{C14})$$

namely a reversed bias where $\overline{\Delta E} > 0$, similar regions can be found by interchanging \rightarrow and \leftarrow . For example, when

$$\overline{\left(\frac{w_a^\rightarrow w_b^\rightarrow}{w_a^\leftarrow w_b^\leftarrow} \right)^2} < 1, \quad (\text{C15})$$

the velocity v and diffusion constant D of the model are finite. Such results of course require that the molecular motors remain attached when they reverse direction.

Note also that the three regimes may be identified (Bouchaud et al., 1990) according to the parameter μ . In particular, we identify $\mu > 2$ with regime I, $1 < \mu < 2$ with regime II, $\mu < 1$ with regime III and $\mu = 0$ with Sinai diffusion.

APPENDIX D: Simple model for the DNA polymerase/exonuclease system

In this appendix a model of the DNA polymerase/exonuclease system is studied. It is shown how a more detailed microscopic model than those studied in the main text also leads to an effective random forcing energy landscape. However, in contrast to these models, the location of the transition points into the anomalous dynamics regime can not be calculated exactly in a straightforward manner.

The model we consider is a simplified version of the model studied by Goel et al. (Goel et al., 2003). The model takes into account the two active sites of the motor, one acting as a polymerase while the other acting as an exonuclease. The system can be in one of five state denoted in Fig. 10 by (a) to (f). The figure represents only transitions which differ by a motion of the motor over a distance of one base. The full model along with an illustration of the experiment is shown in Fig. 11. In state (a) the motor is attached to the ssDNA/dsDNA junction with the polymerase active site. In state (b) the motor uses the energy from the hydrolysis of NTP in order to be able to extend the dsDNA. States (c) and (d) represent similar states but now with the motor connected to the junction using the exonuclease active site. Here the motor does not utilize energy from the hydrolysis of NTP but

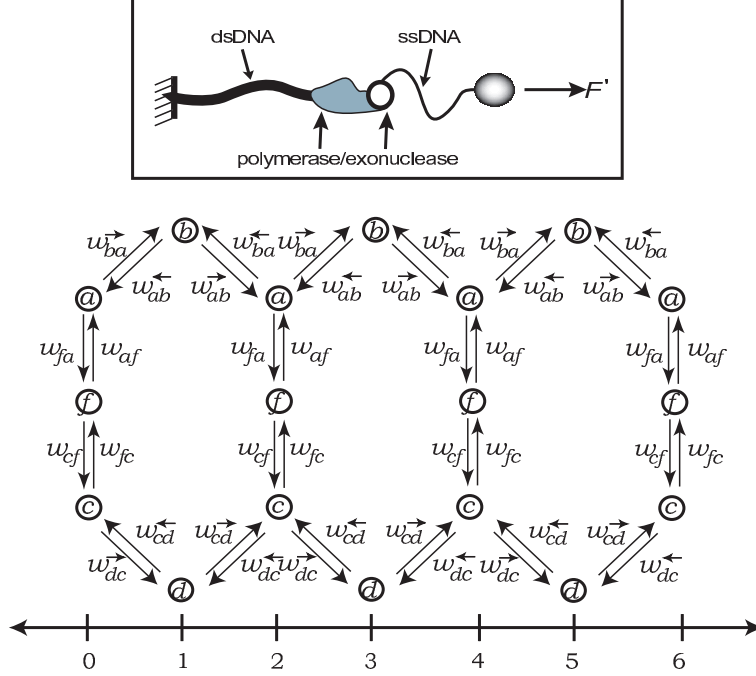


FIG. 11 The full model on the two lane lattice. The inset on the top depicts a cartoon of the experimental system.

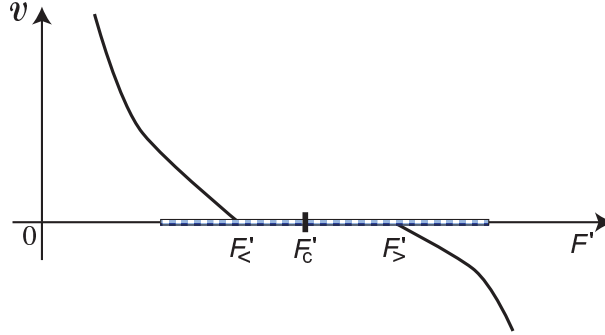


FIG. 12 The expected behavior of the velocity as a function of the external force F of the DNA polymerase / exonuclease system. The striped line represents the region over which the diffusion is expected to be anomalous.

with

$$\begin{aligned}
A = & w_{cf}w_{dc}^{\leftarrow}w_{cd}^{\leftarrow}w_{ba}^{\leftarrow}w_{ba}^{\rightarrow}w_{ab}^{\rightarrow} + w_{af}w_{dc}^{\leftarrow}w_{cd}^{\leftarrow}w_{ba}^{\leftarrow}w_{ba}^{\rightarrow}w_{ab}^{\rightarrow} + w_{af}w_{fc}w_{cd}^{\leftarrow}w_{ba}^{\leftarrow}w_{ba}^{\rightarrow}w_{ab}^{\rightarrow} \\
& + w_{af}w_{fc}w_{cd}^{\rightarrow}w_{ba}^{\leftarrow}w_{ba}^{\rightarrow}w_{ab}^{\rightarrow} + w_{af}w_{cd}^{\rightarrow}w_{dc}^{\leftarrow}w_{ba}^{\leftarrow}w_{ba}^{\rightarrow}w_{ab}^{\rightarrow} + w_{cd}^{\rightarrow}w_{dc}^{\leftarrow}w_{cf}w_{ba}^{\leftarrow}w_{ba}^{\rightarrow}w_{ab}^{\rightarrow} \\
& + w_{cd}^{\rightarrow}w_{dc}^{\rightarrow}w_{fa}w_{cf}w_{ba}^{\rightarrow}w_{ab}^{\rightarrow} + w_{cd}^{\rightarrow}w_{dc}^{\rightarrow}w_{fa}w_{ab}^{\leftarrow}w_{cf}w_{ba}^{\leftarrow}, \tag{D2}
\end{aligned}$$

and

$$B = w_{ab}^{\rightarrow}w_{fa}w_{cf}w_{dc}^{\leftarrow}w_{cd}^{\leftarrow} + w_{ab}^{\leftarrow}w_{fa}w_{cf}w_{dc}^{\leftarrow}w_{cd}^{\leftarrow} + w_{ab}^{\leftarrow}w_{ba}^{\leftarrow}w_{cf}w_{dc}^{\leftarrow}w_{cd}^{\leftarrow} + w_{ab}^{\leftarrow}w_{ba}^{\leftarrow}w_{af}w_{dc}^{\leftarrow}w_{cd}^{\leftarrow}$$

$$\begin{aligned}
& + w_{ab}^{\leftarrow} w_{ba}^{\leftarrow} w_{af} w_{fc} w_{cd}^{\leftarrow} + w_{ab}^{\leftarrow} w_{ba}^{\leftarrow} w_{af} w_{fc} w_{cd}^{\rightarrow} + w_{ab}^{\leftarrow} w_{ba}^{\leftarrow} w_{af} w_{cd}^{\rightarrow} w_{dc}^{\rightarrow} \\
& + w_{ab}^{\leftarrow} w_{ba}^{\leftarrow} w_{cd}^{\rightarrow} w_{dc}^{\rightarrow} w_{cf} .
\end{aligned} \tag{D3}$$

The effective energy landscape can be inferred by assuming an equilibrium distribution so that

$$\frac{P_a(n+2)}{P_a(n)} = \exp((E(n) - E(n+2))/T) , \tag{D4}$$

and the effective energy difference is given by

$$\Delta E = E(n+2) - E(n) = -T \ln \left(\frac{P_a(n+2)}{P_a(n)} \right) . \tag{D5}$$

It is now clear, using Eq. (D1) and arguments similar to those of Sec. IV, that if the set of rates becomes site-dependent, a random forcing energy landscape will develop. The only difference from the simple soluble models studied in the main text is that the random walker representing the system is moving on a two-lane lattice. On general grounds (Fisher, 1984), this will not make a difference on the long time and large length scales behavior of the system. Again, one expects a region when the velocity is anomalous. The expected behavior of the velocity as a function of the external force F' is sketched in Fig. 12. Again, we expect that the singularities at $F'_<$ and $F'_>$ become rounded when v is defined by a finite experimental time window t_E , with a plateau at zero velocity becoming more and more pronounced as $t_E \rightarrow \infty$.

References

- Alexander S., Bernasconi J., Schneider W. R. and Orbach R. 1981. Excitation dynamics in random one-dimensional systems. *Rev. Mod. Phys.* 53:175-198.
- Bhattacharjee S. M. and SenoF. 2003. Helicase on DNA: a phase coexistence based mechanism. *J. Phys. A* 36:L181-L187.
- Bates M., Burns M. and Meller A. 2003. Dynamics of DNA molecules in a membrane channel probed by active control techniques. *Biophys. J.* 84:2366-2372.
- Betterton M. D. and Jülicher F. 2003. A Motor that makes its own track: Helicase unwinding of DNA. *Phys. Rev. Lett.* 91:258103.
- Bianco P. R., Brewer L. R., Corzett M., Balhorn R., Yeh Y., Kowalczykowski S. C. and Baskin R. J. 2001. Processive translocation and DNA unwinding by individual RecBCD enzyme molecules. *Nature.* 409:374-378.

- Bouchaud J. P., Comtet A., Georges A. and Le Doussal P. 1990. Classical diffusion of a particle in a one-dimensional random force-field. *Ann. Phys. (N.Y.)* 201:285-341.
- Bustamante C., Keller D. and Oster G. 2001. The physics of molecular motors. *Acc. Chem. Res.* 34:412-420.
- Chuang J., Kantor Y. and Kardar M. 2002. Anomalous dynamics of translocation. *Phys. Rev. E* 65:011802.
- Coleman J. E. and Oakley J. L. 1980. Physical chemical studies of the structure and function of DNA binding (helix-destabilizing) proteins , *CRC Crit. Rev. Biochem.* 7:247-289.
- Danilowicz C., Coljee V. W., Bouzigues C., Lubensky D. K., Nelson D. R. and Prentiss M. 2003. DNA unzipped under a constant force exhibits multiple metastable intermediates. *Proc. Natl. Acad. Sci.* 100:1694-1699.
- Davenport R. J., Wuite G. J. L., Landick R. and Bustamante C. 2000. Single-molecule study of transcriptional pausing and arrest by E-coli RNA polymerase. *Science* 287:2497-2500.
- Derrida B. 1983. Velocity and diffusion constant of a periodic one-dimensional hopping model. *J. Stat. Phys.* 31:433-450.
- Dohoney K. M. and Gelles J. 2001. chi-Sequence recognition and DNA translocation by single RecBCD helicase/nuclease molecules. *Nature* 409:370-374.
- Doublié S., Tabor S., Long A. M., Richardson C. C. and Ellenberger T. 1998. *Nature* 391:251-258.
- Fisher D. S. 1984. Random walks in random environments. *Phys. Rev. A* 30:960-964.
- Fisher M. E. and Kolomeisky A. B. 1999. The force exerted by a molecular motor. *Proc. Natl. Acad. Sci. USA.* 96:6597-6602; see also Kolomeisky A. B. and Widom B. 1998. A simplified "ratchet" model of molecular motors. *J. Stat. Phys.* 93:633-645.
- Flomenbom O. and Klafter J. 2003. Single stranded DNA translocation through a nanopore: A master equation approach. *Phys. Rev. E* 68:041910.
- Flomenbom O. and Klafter J. 2003. Translocation of a single stranded DNA through a conformationally changing nanopore. *Biophys. J. in press.*
- Gelles J. and Landick R. 1998. RNA polymerase as a molecular motor. *Cell* 93:13-16.
- Goel A., Astumian R. D. and Herschbach D. 2003. Tuning and witching a DNA polymerase motor with mechanical tension. *Proc. Natl. Acad. Sci.* 100:9699-9704.
- Hegner M., Smith S. B. and Bustamante C. 1999. Polymerization and mechanical properties of single RecA-DNA filaments. *Proc. Natl. Acad. Sci.* 96:10109-10114.

- Henrickson S. E., Misakian M., Robertson B and Kasianowicz J. J. 2000. Driven DNA Transport into an Asymmetric Nanometer-Scale Pore. *Phys. Rev. Lett.* 85:3057-3060.
- Howard J. 2001. Mechanics of Motor Proteins and the Cytoskeleton. Sinauer, Sunderland.
- Harms T. and Lipowsky R. 1997. Driven ratchets with disordered tracks. *Phys. Rev. Lett.* 79:2895-2898.
- Jülicher F., Ajdari A. and Prost J. 1997. Modeling molecular motors. *Rev. Mod. Phys.* 69:1269-1281.
- Jülicher F. and Bruinsma R. 1998. Motion of RNA polymerase along DNA: A stochastic model. *Biophys. J.* 74:1169-1185.
- Kasianowicz J. J., Brandin E., Branton D. and Deamer D. W. 1996. Characterization of individual polynucleotide molecules using a membrane channel. *Proc. Natl. Acad. Sci. USA.* 93:13770-13773.
- Kolomeisky A. B. and Fisher M. E. 1999. A simple kinetic model describes the processivity of myosin-V. *Biophys. J.* 84:1642-1650.
- Kowalczykowski S. C., Lonberg N., Newport J. W. and von Hippel P. H. 1981. Interactions of bacteriophage T4-coded gene 32 protein with nucleic-acids .1. characterization of the binding interactions. *J. Mol. Biol.* 145:75-104.
- Lattanzi G. and Maritan A. 2001. Force dependence of the Michaelis constant in a two-state ratchet model for molecular motors, *Phys. Rev. Lett.* 86:1134-1137.
- Lattanzi G. and Maritan A. 2001. Master equation approach to molecular motors, *Phys. Rev. E* 64:061905.
- Lattanzi G. and Maritan A. 2002. Force dependent transition rates in chemical kinetics models for motor proteins, *J. Chem. Phys.* 117:10339-10349.
- Landau L. D. and Lifshitz E. M., *Statistical Physics, Part 1*, 3rd Edition (Pergamon, New York).
- Lohman T. M. and Bjornson K. P. 1996. Mechanisms of helicase-catalyzed DNA unwinding. *Ann. Rev. Biochem.* 65:169-214.
- Lubensky D. K. and Nelson D. R. 1999. Driven polymer translocation through a narrow pore. *Biophys. J.* 77:1824-1838.
- Lubensky D. K. and Nelson D.R. 2000. Pulling pinned polymers and unzipping DNA. *Phys. Rev. Lett.* 85:1572-1575.
- Lubensky D. K. and Nelson D. R. 2002, Single molecule statistics and the polynucleotide unzipping transition. *Phys. Rev. E* 65:031917.
- Maier B., Bensimon D. and Croquette V. 2000. Replication by a single DNA polymerase of a

- stretched single-stranded DNA. *Proc. Natl. Acad. Sci. USA*. 97:12002-12007.
- Magnasco M. O. 1993. Forced thermal ratchets. *Phys. Rev. Lett.* 71:1477-1481.
- Meller A. 2003. Dynamics of polynucleotide transport through nanometre-scale pores. *J. Phys: Condens. Matter*. 15:R581-R607.
- Meller A., Nivon L. and Branton D. 2001. Voltage-driven DNA translocations through a nanopore. *Phys. Rev. Lett.* 86:3425-3438.
- Muthukumar M. 2001. Translocation of a confined polymer through a hole. *Phys. Rev. Lett.* 86:3188-3191.
- Nelson P. 2003. *Biological Physics: Energy, Information, Life* (W. H. Freeman and Co., New York, 2003).
- Newport J. W., Lonberg N., Kowalczykowski S. C. and von Hippel P. H. 1981. Interactions of bacteriophage T4-coded gene 32 protein with nucleic-acids .2. specificity of binding to DNA and RNA. *J. Mol. Biol.* 145:105-121.
- Prost J., Chauwin J.-F., Peliti L. and Ajdari A. 1994. Asymmetric pumping of particles. *Phys. Rev. Lett.* 72:2652-2655.
- Peskin C. S., Odell G. M. and Oster G. F. 1993. Cellular motions and thermal fluctuations - the brownian ratchet. *Biophys. J.* 65:316-324.
- SantaLucia J., A unified view of polymer, dumbbell, and oligonucleotide DNA nearest-neighbor thermodynamics. *Proc. Natl. Acad. Sci. USA* 95:1460-1465.
- Simon S. M., Peskin C. S. and Oster G. F. 1992. What drives the translocation of proteins. *Proc. Natl. Acad. Sci. USA*. 89:3770-3774.
- Sinai Ya. G. 1982. *Lecture Notes in Physics No. 153* (Springer, Berlin, 1982), p. 12.
- Smith S. B., Cui Y., and Bustamante C. 1996. Overstretching B-DNA: The elastic response of individual double-stranded and single-stranded DNA molecules. *Science* 271:795-799.
- Smith D. E., Tans S. J., Smith S. B., Grimes S., Anderson D. L. and Bustamante C. 2001. The bacteriophage phi 29 portal motor can package DNA against a large internal force. *Nature*. 413:748-752.
- Sung W. and Park P. J. 1996. Polymer translocation through a pore in a membrane. *Phys. Rev. Lett.* 77:783-786.
- Visscher K., Schnitzer M. J. and Block S. M. 1999. Single kinesin molecules studied with a molecular force clamp. *Nature*. 400:184-189.

- von Hippel P. H. and Delagouette E. 2001. A general model for nucleic acid helicases and their "coupling" within macromolecular machines. *Cell* 104:177-190.
- von Hippel P. H. and Pasmán Z. 2002. Reaction pathways in transcript elongation. *Biophys. Chem.* 101:401-423.
- Wang M. D., Schnitzer M. J., Yin H., Landick H., Gelles H. and Block S. M.. 1998. Force and velocity measured for single molecules of RNA polymerase. *Science.* 282:902-907.
- Wuite G. J. L., Smith S. B., Young M., Keller D. and Bustamante C. 2000. Single-molecule studies of the effect of template tension on T7 DNA polymerase activity. *Nature.* 404:103-106.
- Zandi R., Reguera D., Rudnick J. and Gelbart W. M. 2003. What drives the translocation of stiff chains? *Proc. Natl. Acad. Sci.* 100:8649-8653.